Drosophila Toll links systemic immunity to long-term intestinal epithelial integrity.

Magda L. Atilano[1,2], Marcus Glittenberg[2], Anna Hoyle and Petros Ligoxygakis

Laboratory of Cell Biology, Development and Genetics, Department of Biochemistry, University of Oxford, South Parks Rd OX1 3QU Oxford UK.

[1]Present address: Institute for Healthy Aging, University College London, Gower Street WC1E 6BT, London UK.

[2]These authors contributed equally to this work

Corresponding author: petros.ligoxygakis@bioch.ox.ac.uk

The intestine is an organ where immune, metabolic and neuroendocrine regulation is coordinated with the rapid renewal of the tissue via progenitor somatic stem cells (PSSCs). However, how these cells are influenced by each of the different physiological activities of the intestine is still unclear. We report here that in *Drosophila,* systemic infection significantly increased PSSC numbers, which was mimicked by expressing a constitutive form of the immune receptor Toll in PSSCs and blocked when Toll was silenced via RNAi. Toll was important for the transition of Intestinal Stem Cells (ISCs) to Enteroblasts (EBs) and Toll silencing in either in the absence of infection resulted in the long-term reduction of PSSC numbers. This phenotype was also observed in mutants of the Peptidoglycan Recognition Protein-SA (PGRP-SA), acting upstream of Toll. PGRP-SA mutations or Toll-RNAi in progenitor cells led to a marked decrease in gut microbiota, implying that a regularly renewed intestine was crucial for maintenance of normal numbers of commensal bacteria. Infection or constitutive Toll signalling in progenitor cells triggered FOXO-dependent transcription in enterocytes. Our results show that PGRP-SA-Toll immunity is crucial for gut homeostasis.

Introduction: Innate immunity is the first-line host defence conserved in all metazoans (reviewed in Akira and Takeda 2004). In this context, Toll-like receptor (TLR) signalling is one of the most important mechanisms by which the innate immune system senses the invasion of pathogenic microorganisms in both mammals and *Drosophila.* Unlike its mammalian counterparts however, the fly Toll is activated by an endogenous cytokine-like ligand, the Nerve Growth Factor homologue, Spz (Weber *et al,* 2003). The latter is processed to its active form by the Spz-processing enzyme (SPE) (Jiang *et al*, 2006). Two serine protease cascades converge on SPE: one triggered by bacterial or fungal serine proteases and a second activated by host proteins that recognise bacterial or fungal cell wall. Prominent among these host proteins is Peptidoglycan Recognition Protein-SA (PGRP-SA) (Michel *et al,* 2001). When transduction of the recognition signal reaches the Toll receptor, it is

37 communicated to the nucleus through a receptor-adaptor complex including Myd88 and IRAK4-
38 homologues and culminates in the phosphorylation of the IκB homologue, Cactus (reviewed in
39 Kounatidis and Ligoxygakis, 2012). This modification targets Cactus for degradation, leaving the NF-
40 κB homologue DIF to move to the nucleus and regulate hundreds of target genes including a battery
41 of powerful antimicrobial peptides (AMPs) (de Gregorio *et al*, 2002).

42 As in mammals, the high capacity of intestinal epithelial regeneration in flies depends on
43 intestinal stem cells (ISCs). As in mammals, tissue homeostasis in the fly gut is maintained by
44 multipotent ISCs, which are distributed along the basement membrane of the posterior midgut
45 (Ohlstein and Spradling 2006; Ohlstein and Spradling 2007, reviewed in Lemaitre and Miguel-Aliaga,
46 2013). There, an ISC divides to produce itself and an enteroblast (EB), which will undergo terminal
47 differentiation into an enterocyte (EC) or an enteroendocrine cell (EE). Progenitor cells (ISCs and EBs)
48 express a transcription factor called Escargot (*esg*) (Ohlstein and Spradling 2006; Ohlstein and
49 Spradling 2007; Amcheslavsky *et al* 2009). Thus, expression of *esg* is often used as a surrogate
50 marker for studying both ISCs and EBs in the anterior midgut (Fig. 1A). In the present work, we
51 investigated how systemic infection triggering Toll may be linked to long-term intestinal
52 homeostasis.

53

54 **Results and discussion:** Systemic infection of 20-day old adults expressing GFP under the *esg*
55 promoter, with the opportunistic fungal pathogen *Candida albicans* (*C. albicans*), resulted in a
56 statistically significant increase of GFP-positive cells (Fig. 1B). This result indicated that systemic
57 immunity regulated progenitor cell numbers. Since Toll is the pathway primarily responding to fungal
58 infections in *Drosophila,* we attempted to reproduce the result by mimicking Toll triggering by
59 infection. To this end, we expressed a constitutively active form of Toll (Toll10B) in *esg*-expressing
60 cells with the GAL4-UAS system. Indeed, this resulted again in a significant increase of large GFP
61 positive cells reminiscent of EBs (Fig. 1C). To identify if this was indeed an increase in EBs we

62 expressed UAS-Toll10B with Su(H)-GAL4 (an EB-specific GAL4; Ohlstein and Spradling 2006; Ohlstein
63 and Spradling 2007). We observed a significant rise in the numbers of EBs [Su(H)-GAL4] (Fig. 1C).
64 Taken together, the above data indicated that Toll signalling was sufficient in influencing the pool of
65 progenitor cells towards the EB fate or expanding the numbers of existing EB cells.

66 We next asked whether, in addition to being sufficient, Toll was also necessary for
67 controlling intestinal epithelial renewal following fungal infection using the GAL4/GAL80^{ts} system
68 (Suster *et al*, 2004). We silenced Toll in progenitor cells using *esg-GAL4, UAS-GFP GAL80^{ts}; UAS-*
69 *Toll^{RNAi}* (*esg^{ts}>Toll^{RNAi}*). The whole of development proceeded at the permissive temperature of 18^{o}C
70 (GAL80 ON, GAL4 OFF, Toll ON). Then, one-day old adults were transferred to the restrictive
71 temperature of 30^{o}C (GAL80 OFF, GAL4 ON, Toll OFF) and infected with *C. albicans* 20 days later.
72 After infection we examined the number of GFP-positive cells 36h post-infection. Following the same
73 protocol we used as a control for the RNAi mechanism a line from the VDRC collection (UAS-
74 CG7923^{RNAi}) that did not compromise host survival when infected with *C. albicans* and exhibited a
75 normal lifespan compared to its genetic background in the absence of infection (data not shown;
76 based on a targeted genetic screen using host survival after *C. albicans* infection as read-out,
77 Glittenberg *et al* in preparation). In these control flies, there was a statistically significant increase in
78 GFP-positive cells comparing sterile injury (PBS) with septic injury (*C. albicans*) as seen in Fig. 2A (and
79 quantified in Fig. 2B). In contrast, silencing Toll prevented this increase in progenitor cells as GFP-
80 positive cells were statistically inseparable following PBS injection vs. *C. albicans* infection (Fig. 2C;
81 quantified in Fig. 2B). Moreover, we noted that the number of GFP positive cells in *esg^{ts}>UAS-*
82 *CG7923^{RNAi}* flies was higher than in *esg^{ts}>UAS-Toll^{RNAi}* after PBS treatment, raising the possibility that
83 the *esg^{ts}>UAS-Toll^{RNAi}* had less progenitor cells in the steady state of 20-day old adults (Fig. 2B).

84 To test long-term renewal of the intestinal epithelium in the absence of infection, we
85 assayed guts from 6-day old and 20-day old *esg^{ts}>UAS-Toll^{RNAi}* flies and compared them to
86 chronologically age-matched *esg^{ts}>UAS-CG7923^{RNAi}* controls. We found that compared to *esg^{ts}>UAS-*

87 *CG7923*^{RNAi}, the shape of GFP positive progenitor cells in guts of *esg*^{ts}*>UAS-Toll*^{RNAi} adults was
88 significantly altered with cells becoming smaller and more rounded at 20 days (Fig. 3A). They were
89 also significantly reduced in numbers (Fig. 3B), with the guts becoming extremely fragile to handle
90 (hence the slightly lower total number of *esg*^{ts}*>UAS-Toll*^{RNAi} guts in the graph). Moreover, cultivable
91 intestinal microbiota were significantly lower at 20-days as measured by CFUs (Fig. 3C). The same
92 effect in cell shape at 20 days was also observed when Toll was silenced using the EB-specific Su(H)-
93 GAL4 in a *Su(H)*^{ts}*>UAS-Toll*^{RNAi} configuration (Fig. S1). Taken together, results in Figs 1-3 showed that
94 Toll was both necessary and sufficient for regulating the long-term regeneration potential of the
95 intestine after an immune challenge but also in the absence of infection.

96 Flies mutant for the upstream Toll pathway component namely, *PGRP-SA*^{seml} (Michel *et al*,
97 2001) also showed a reduction in ISCs dividing to EBs (Fig 4A) and a significant reduction in the
98 numbers of both ISCs in particular and progenitor cells in general (Fig. 4B). However, expression of
99 Toll10B in *PGRP-SA*^{seml} progenitor cells was able to reconstitute ISCs in the anterior midgut (Fig. S2A)
100 in numbers statistically indistinguishable from the *yw,* genetic background (Fig. S2B). Notably, *PGRP-*
101 *SA*^{seml} mutants had a markedly reduced intestinal microbiota in the cultivable component as
102 measured by Colony Forming Units (CFUs) (Fig. 5). Reduction in CFUs was independent of the genetic
103 background of the PGRP-SA mutation as it was observed when the *PGRP-SA*^{seml} mutation was
104 transferred to one of the DGRP (*Drosophila* Genetics Reference Panel) lines (strain 25174) (Fig 5). Of
105 note that in *dif* mutants, CFU reduction was more pronounced with age underlying the long-term
106 influence of the loss of Toll signalling (Fig. 5).

107 This brought forward the possibility that maintenance of the regenerative potential of the
108 gut through the PGRP-SA-Toll-DIF signal was important to preserve a normal load of intestinal
109 microbiota. Of course, the reverse was also a valid hypothesis: loss of PGRP-SA could cause
110 microbiota reduction that in turn provoked intestinal progenitor. To distinguish between these two
111 alternative scenarios we based our reasoning on two recent reports establishing that rapamycin was

able to maintain the long-term regenerative potential of the intestine through inhibition of the Target of Rapamycin Complex 1 (mTORC1) (Fan *et al,* 2015; Haller *et al*, 2017). Indeed, administration of 200μM rapamycin to 20-day old *ywPGRP-SA*^{seml} mutant flies, was able to expand the presence of progenitor cells in the anterior midgut (Fig. 6A) with a significant increase in numbers compared to the vehicle control (Fig. 6B). Moreover, rapamycin was able to restore microbiota density to the levels of the *yw* genetic background (Fig. 6C). In turn, this strongly suggested that loss of PGRP-SA-Toll signalling led to an increase in mTORC1 activity, which generated an intestinal metabolic environment leading to an age-dependent microbiota decrease.

Given the above, we wanted to analyse further how Toll signalling in progenitor cells may provoke metabolic changes in the gut. In this context, a major determinant of metabolic status and an antagonist for some of mTORC1-mediated outcomes is the *Drosophila* Fork Head Box O (FOXO) transcription factor (Puig *et al,* 2003; Jia *et al*, 2004; Chen *et al* 2010; Artoni *et al*, 2017). Using quantitative real time PCR, we tested the effects of *esg-GAL4*-mediated overexpression of *UAS-Toll*^{RNAi} or *UAS-Toll10B* on FOXO dependent transcription. Comparing to expression of a *UAS-RFP* control, Toll knock down in progenitor cells significantly increased expression of the insulin receptor (*InR*) and the *Drosophila* insulin peptide-3 (*dilp3*) as well as FOXO itself (Fig. S3A). Conversely, constitutive expression of Toll significantly downregulated expression of *InR, dilp3* and FOXO (Fig. S3A). We reckoned that these changes would not be a result of difference in progenitor cells (since there are too few and our method was not sensitive enough to detect them) but in ECs. A marker of FOXO transcription under stress conditions (starvation, oxidative stress) is *Thor* the fruit fly homologue of the eukaryotic translation initiation factor 4 (4E-BP) (Tettweller *et al*, 2005). Indeed, *C. albicans*-infected flies increased *thor* transcription (measured by qPCR) but not when subjected to FOXO RNAi with the enterocyte- specific *NP1-GAL4* (Fig. S3B). At the tissue level, systemic infection of *C. albicans*, had a *Thor-lacZ* construct upregulated in their ECs (Fig. 7A, quantification in Fig. 7B). This upregulation in ECs could be reproduced when *UAS-Toll10B* expression was driven by *esg-GAL4* in progenitor cells (Fig. 8A, quantification in Fig. 8D). Effects on FOXO-dependent transcription in

138 *esg^{ts}>UAS-Toll10B* were microbiota-independent since germ-free flies showed a similar activation of
139 *Thor-LacZ* (our unpublished observations), reinforcing the idea that the effects observed when Toll
140 was constitutively active in progenitor cells were intrinsic to the tissue and these then influenced the
141 gut microbiota.

142 Long-term intestinal regeneration is important for preserving organ function. In mice, the
143 presence of TLR4 has been linked to increased proliferation of ISCs (Neal *et al*, 2012). However, the
144 effect of the absence of TLRs has been less clear. Our results show that following infection as well as
145 under homeostatic conditions, absence of Toll signalling blocked ISC-to-EB transition and reduced
146 the load of gut microbiota. These phenotypes were alleviated by using rapamycin, which targets
147 mTORC1 (reviewed in Laplante and Sabatini, 2012). This result showed that absence of Toll signalling
148 triggered mTORC1. It has been shown that an increase in mTORC1 signalling elevates glycolytic flux
149 and energy consumption, promoting anabolic processes and thus changing the cellular metabolic
150 profile forcing an "anabolic state" (Laplante and Sabatini, 2012). We speculate that this altered the
151 metabolic profile of the gut, starving bacteria from catabolic products (and thus reducing microbiota
152 density) as well as halting ISC division. One component of the Toll pathway important for its function
153 to preserve long-term intestinal progenitor numbers was the bacterial receptor PGRP-SA. It is
154 tempting to speculate that PGRP-SA recognises parts of the flora and as such activates the pathway,
155 which in turn keeps mTORC1 low and thus preserves a catabolic state favourable for normal
156 microbiota density. In this context, PGRP-SA function resembles intestinal TLR-2, Myd88-mediated
157 responses in the T-cell compartment of the mouse gut (Kubinak *et al,* 2015). More work is needed to
158 pinpoint, which constituent(s) of the microbiota PGRP-SA may recognise.

159 Toll signalling either in constitutive form or through *C. albicans* infection activated FOXO-
160 dependent transcription in ECs including *InR, dilp3* and *Thor*. Insulin pathway activity has been
161 shown to suppress FOXO-mediated transcription. DiAngelo *et al*, 2009 described how the activation
162 of the Toll pathway in the fat body leads to a suppression of insulin signalling as a mechanism to

preserve energy during infection. Since *Thor* is activated following infection as well as Toll constitutive signalling, our results would suggest the mechanism may well be conserved in other organs, such as the gut as the balance between nutrient availability and infection is necessary in any part of the organism. Nevertheless, more work is needed to determine the signal by which Toll signalling is communicated from the progenitor cells to ECs.

Our data support a model where systemic immunity to infection is directly linked to epithelial renewal through the evolutionary conserved Toll receptor, which in this manner ties together the immune and metabolic aspects of intestinal physiology with long-term epithelial homeostasis.

Materials and Methods: *Fly strains* we used the *yw* and 25174 DGRP strain as genetic background controls. We incorporated the PGRP-SA^{seml} mutation in 25174 and *esg^{ts}>GAL4* (Buchon *et al*, 2009). We also incorporated UAS-CG7923^{RNAi}, UAS-9080^{RNAi} and UAS-Toll^{RNAi} in *esg^{ts}>GAL4.* All RNAi strains were obtained from the Vienna Stock Centre (Dietzl *et al*, 2007). *Thor-lacZ* (y',w*; p{lacW}Thor^{K13517}) was obtained from Bloomington Stock Centre IN USA. For Toll constitutive expression we used *UAS-Toll10B* (Shia *et al*, 2009).

Infection To infect flies, *Candida albicans (C. albicans)* strain was cultured in Sabouraud's glucose broth (SGB; Oxoid) for 18 hours; cells were harvested by centrifugation (3200 rpm for 5 minutes) and washed in sterile phosphate buffered saline (PBS). Washed fungal cells were again centrifuged and re-suspended in PBS to an optical density of approximately 0.95-1.05 (Thermo Scientific NanoDrop 1000 spectrophotometer). The inoculant containing *C. albicans strain* was further diluted 4 fold in PBS. Anaesthetized female flies (aged 10-12 days) were infected with 13.2nl of yeast cells suspension (or with PBS control), directly injected into the haemolymph through the dorsolateral region of the thorax, using a micro-injector (Drummond Scientific Nanoinject II). The number of viable yeast cells injected per fly was approximately 600, as calculated from plating homogenates of six injected flies, previously ground in SGB medium. Flies were kept at 30°C post-infection for 36 hours and then dissected.

Gut dissection and immunostaining For gut imaging, guts from anesthetized flies were dissected in Schneider's medium and fixed for 30-40 min in 4% paraformaldehyde (in PBS), rinsed in PBS and then three times (5 min each) in wash solution, 0.1% Triton X-100 (Sigma-Aldrich) in PBS. The tissue was blocked overnight at 4°C in blocking solution (0.1% Triton X-100, 2% BSA (Sigma-Aldrich) in PBS. For immunofluorescence, the guts were incubated with primary antibody dilution 1:100 mice anti-β-galactosidase (40-1a-S, Developmental Studies Hybridoma Bank, Iowa, USA) and then washed 4x in wash solution 15 min each. The primary antibody was revealed with 1:250 donkey anti-mouse Alexa-568 antibody (Invitrogen), and nuclei were stained with DAPI 1:1000 (Sigma-Aldrich). Washed guts

were mounted in slides with vectorshield mounting media (Vector Laboratories). Guts were then scanned with in an Axioplot imager (Zeiss) and analysed using the ImageJ program.

X-GAL (LacZ) staining of the gut Following dissection in Schneider solution tissue was fixed in paraformaldehyde, 4%, (diluted from 16% stock, VWR) and left for 45 minutes. Tissue was washed three times with wash solution (2mM $MgCl_2$ in PBS), 15 minutes each. X-Gal reaction buffer containing: 35mM potassium ferrocyanide (Sigma-Aldrich), 35mM potassium ferricyanide (Sigma-Aldrich), 2mM $MgCl_2$ (Sigma-Aldrich), 0.1% Triton and X-Gal (1mg/ml) in PBS was then added to the tissue and incubated overnight with gentle agitation. Finally the tissue was rinsed several times with PBS until the solution no long turned yellow (approximately five times). Tissue was then mounted as mentioned before and viewed under bright field optics.

RNA extraction and quantitative real-time PCR Flies were dissected as described above but then the crop and hindgut were removed and the guts were placed in an Eppendorf tube. Fifteen guts were dissected for each condition/strain. The total RNA was isolated using the Norden Biotek Corp. Total RNA isolation kit. This involved removing the Schneider solution from the tube and replacing it with lysis buffer (300ul) provide by the kit. The guts were then homogenised using a needle attached to a homogeniser to burst all the guts. The remaining protocol was performed according to the manufacturer's instructions. The purity and the concentration of the RNA samples were checked using the NanoDrop 1000 spectrophotometer (Thermo Scientific), and 500ng of RNA was reverse transcribed into cDNA with the Maxima First Strand cDNA Synthesis kit (ThermoFisher Scientific) according to the manufacturer's instructions. The reaction conditions involved a step at 25°C for 10 min followed by a 15 minute step at 65°C and ending with a 5 min step at 85° C. For the quantitative PCR (qPCR) the levels of the cDNA for InR, Drs, Foxo, Rheb, Dilp3, AMPK were measured, as were the levels of the cDNA for the TATA binding protein (TBP). The TBP measurement was used as a control to normalise the expression of the genes of interest. qPCR reactions (SensiFast SYBR No-ROX Kit, Bioline, UK) were carried out using 2 microliters of cDNA template diluted tenfold and 400nM of

each primer (see supplementary table for primer sequence) in a Rotor-Gene Q real-time PCR cycler with a 72-well rotor (Qiagen). The gene expression was calculated according to the comparative threshold cycle (CT) value.

Microbiota analysis at the indicated age-points (Fig. 3C, Fig. 5 and Fig. S2), six female flies from each of three different vials, each containing approximately 20 flies, were assayed for total microbiota load. The microbiota load was determined both by plating fly extracts and by PCR amplification of the 16S ribosomal RNA gene from DNA obtained from dissected guts. The remaining flies were transferred to fresh vials every two days. Flies were first washed with cold ethanol (70%) and then rinsed in PBS. Flies were homogenized in M.R.S broth, the extract dilutions were then spread on M.R.S agar and the plates were incubated at 30°C. After 48 hours, colonies were counted. For PCR assay, total DNA was extracted from dissected midguts (crop and hindgut were removed) using a 21-G hypodermic needle attached to a homogenizer and the Cells and Tissue DNA Isolation Kit (NORGEN). The 16S region PCR amplification was carried out for 10 nanograms of each DNA sample, using 50-µl reaction mixtures. Each reaction mixture contained 0.5µM of each primer (see supplementary table for primer sequence), a 200 µM concentration of each deoxynucleoside triphosphate (dNTP), and 1µM Phusion *Taq* polymerase (New England Biolabs). The PCR conditions involved an initial denaturation step at 98°C for 30 sec followed by 35 cycles of 95°C for 30 sec, 65°C for 30 sec, and 72°C for 1 min and ended with an extension step at 72°C for 5 min in a thermocycler (T100 thermal cycler, Bio-Rad). PCR samples were run in a 0.8% agarose gel. The gel was stained with ethidium bromide, visualized and digitally photographed by Alphalimager HP Gel (Alpha Innotech) imaging system. The bands intensities were analysed in Image J (Grigoryan, Grigoryan 2013).

Germ free flies for collecting embryos, male and female flies were placed in a fly cage and were allowed to lay eggs on apple juice agar plates over 3 hours. To ensure complete removal of extracellular bacteria from the eggs, an ethanol–based protocol was chosen. Embryos were

collected and dechorionated for 2 min in 2.7% sodium hypochlorite solution, then washed twice in 70% ethanol and then twice with sterile, distilled water as was described by (Bouchon *et al,* 2009). Embryos were then moved to sterile food without antibiotics and allowed to develop. The bleach, ethanol and water steps were avoided in the control experiments to exclude the possibility that it might influence the number of microbiota on the eggs. All manipulations of the axenic flies (bacterial depleted) were performed near a flame to prevent contamination. Furthermore, vials and bottles containing dechorionated flies were monitored for the characteristic developmental delay phenotypes of bacterial-depleted flies and the depletion of bacteria from emerged axenic flies were assayed by plating cell extracts.

Statistical analysis Data was analysed using GraphPad Prism 6 or R. First a D' Agostino and Pearson omnibus Normality test was conducted. If the data was found to fit a normal distribution, parametric tests were used, first a 2 was ANNOVA and then a Tukey's multiple comparisons test. The data did not fit the normal distribution in the cases of the Thor-LacZ and the GFP count data. GraphPad was used to conduct a Kruskal-Wallis test for the Thor-LacZ data followed by the Dunn's multiple comparisons test to clarify the significance these tests used the median and the interquartile range. R was used to analyse the GFP count data, it was fitted to a generalised linear model using a quasi-Poisson regression and then ANNOVA and Tukey's multiple comparisons tests were employed to look for significance.

Acknowledgements: We would like to thank the Vienna and Bloomington Stock Centres, as well as Bruno Lemaitre for fly stocks and the Iowa Hybridoma Bank for antibodies. This work was funded by ERC Consolidator Grant 310912 and BBSRC Responsive Mode Grant BB/P005691/1 (both to PL).

References: Akira S and Takeda K (2004). Toll-like receptor signalling *Nature Reviews Immunology* **4**, 499–511.

Amcheslavsky A, Jiang J, Ip YT (2009). Tissue damage-induced intestinal stem cell division in *Drosophila*. *Cell Stem Cell* **4**, 49-61.

Artoni F, Kreipke RE, Palmeira O, Dixon C, Goldberg Z *et al* (2017). Loss of *foxo* rescues stem cell aging the in the *Drosophila* germ line. *eLife* **6,** e27842.

Buchon N, Broderick NA, Chakrabarti S, Lemaitre B (2009). Invasive and indigenous microbiota impact intestinal stem cell activity through multiple pathways in *Drosophila*. *Genes Dev.* **23,** 2333-2344.

Chen CC, Jeon SM, Bhaskar PT, Nogueira V, Sundararajan D, *et al* (2010). FoxOs inhibit mTORC1 and activate Akt by inducing the expression of Sestrin3 and Rictor. *Dev Cell* **18,** 592-604.

De Gregorio E, Spellman PT, Tzou P, Rubin GM, Lemaitre B (2002) The Toll and Imd pathways are the major regulators of the immune response in *Drosophila*. *EMBO J*, **21**, 2568-2579.

DiAngelo JR, Bland ML, Bambina S, Cherry S, Bimbaum MJ (2009). The immune response attenuates growth and nutrient storage in *Drosophila* by reducing insulin signalling. *Proc Acad Sci USA* **106,** 20853-20858.

Dietzl G, Chen D, Schnorrer F, Su KC, Feliner M *et al* (2007). A genome-wide transgenic RNAi library for conditional gene inactivation in *Drosophila*. *Nature* **448,** 151-156.

Fan X, Liang Q, Lian T, Wu Q, Gaur U *et al* (2015). Rapamycin preserves gut homeostasis during *Drosophila* aging. *Oncotarget* **6,** 35274-35283.

Haller S, Kapuria S, Riley RR, O'Leary MN, Schreiber KH *et al* (2017). mTORC1 activation during repeated regeneration impairs somatic stem cell maintenance. *Cell Stem Cell* **21**, 806-818.

Jia K, Chen D, Riddle DL (2004). The TOR pathway interacts with the insulin signalling pathway to regulate *C. elegans* larval development, metabolism and lifespan. *Development* **131,** 3897-3906.

Jiang I-H, Chosa N, Kim S-H, Nam H-J, Lemaitre B *et al* (2006). A Spätzle-processing enzyme required for Toll signalling activation in *Drosophila* innate immunity. *Dev Cell* **10,** 45-55.

Kounatidis I and Ligoxygakis P (2012). *Drosophila* as a model system to unravel the layers of innate immunity to infection. *Open Biology* **doi: 10.1098/rsob.120075**

Kubinak JL, Petersen C, Stephens WZ, Soto R, Bake E *et al* (2015) Myd88 signalling in T-cells directs IgA-mediated control of the microbiota to promote health. *Cell Host & Microbe* **17,** 153-163**.**

Laplante M, Sabatini DM (2012) mTOR signalling in growth control and disease. *Cell* **149**, 274-293.

Lemaitre B, Miguel-Aliaga I (2013). The digestive tract of *Drosophila melanogaster*. *Annu Rev Genet.* **47**, 377-404.

Michel T, Reichhart J-M, Hoffmann JAH, Royet J (2001). *Drosophila* Toll is activated by Gram-positive bacteria through a circulating peptidoglycan recognition protein. *Nature* **414**, 756–759.

Neal MD, Sodhi CPS, Hongpeng J, Dyer M, Egan CE *et al* (2012) Toll-like Receptor 4 Is Expressed on Intestinal Stem Cells and Regulates Their Proliferation and Apoptosis via the p53 Up-regulated Modulator of Apoptosis. *Journal of Biological Chemistry* ***287,*** 37296-37308.

Ohlstein B, Spradling A (2006). The adult *Drosophila* posterior midgut is maintained by pluripotent stem cells. *Nature* **439**, 470-474.

Ohstein B, Spradling A (2007). Multipotent *Drosophila* intestinal stem cells specify daughter fates by differential Notch signalling. *Science* **315**, 9880992.

Puig O, Marr MT, Ruhf ML, Tijan R (2003). Control of cell number by *Drosophila* FOXO: downstream and feedback regulation of the insulin receptor pathway. *Genes & Dev* **17,** 2006-2020.

316 Shia AKH, Glittenberg M, Thompson G, Weber AN, Reichhart J-M, Ligoxygakis P (2009). Toll-
317 dependent antimicrobial responses in *Drosophila* larval fat body require Spaetzle secreted by
318 haemocytes. *J Cell Sci.* **122**, 4505-4515.

319 Suster ML, Seugnet L, Bate M, Sokolowski MB (2004). Refining GAL4-driven transgene
320 expression in *Drosophila* with a GAL80 enhancer trap. *Genesis* **39**, 240-245.

321 Tettweller G, Miron M, Jenkins M, Sonenberg N, Lasko PP (2005). Starvation and oxidative
322 stress resistance in *Drosophila* are mediated through the eIF4E-binding protein, d4E-BP. *Genes Dev*
323 **19,** 1840-1843.

324 Weber AN, Tauszig-Delamasure S, Hoffmann JAH, Lelievre E, Gascan H *et al* (2003). Binding
325 of *Drosophila* cytokine Spaetzle to Toll is direct and established signalling. *Nature Immunology* **4**,
326 794–800.

327

328

329

330

331 **FIGURE 1**

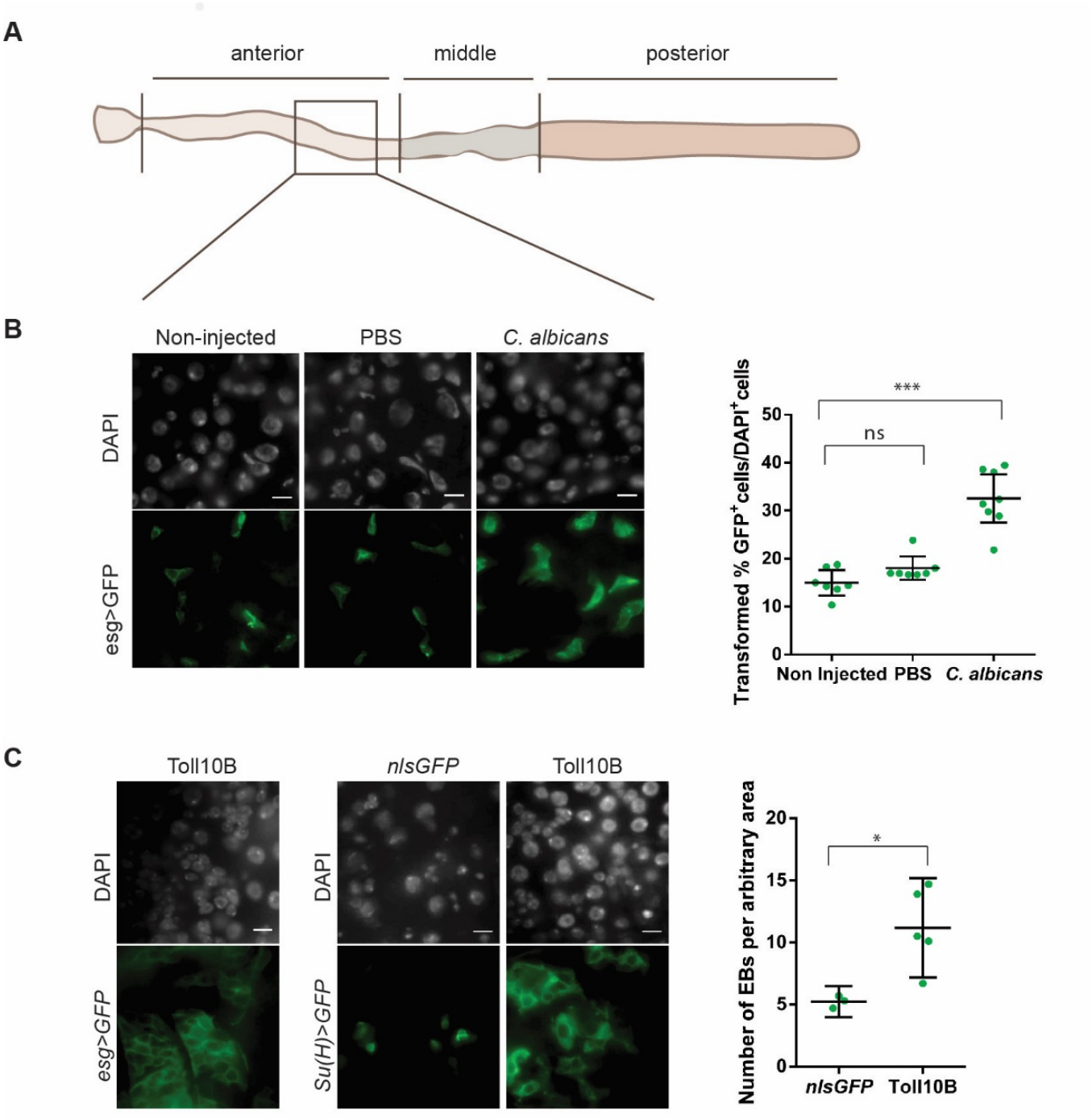

332

333 **FIGURE 1: Progenitor cells respond to systemic *C. albicans* infection.** Focusing on an area of the
334 anterior midgut close to the border with the middle midgut **(A)** we found a significant increase in
335 large GFP-positive cells (green) found in *esg>GFP* intestines following injection of *C. albicans* in the
336 thorax compared to sterile injury with PBS **(B).** This was mimicked in the absence of infection or
337 injury by the expression of a constitutively active form of the Toll receptor (Toll10B) when expressed

in progenitor cells (esg-GAL4) or just in EBs [Su(H)-GAL4] and compared to expression of nlsGFP **(C).** This implied that the large GFP cells seen in (B) were EBs. All nuclei were stained with DAPI (grey). In the plots, each dot represents the counted area from a single gut; 95% confidence interval is displayed (***p<0.001, *p<0.1, ns=non-significant).

FIGURE 2

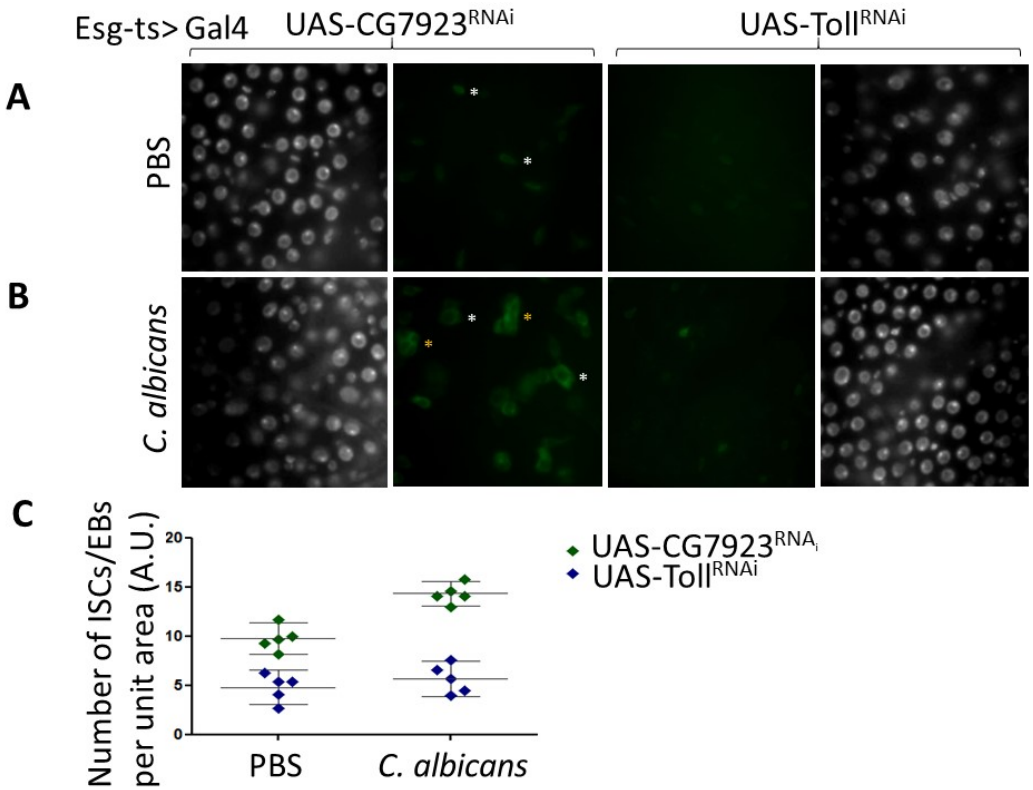

Figure 2: Silencing Toll in intestinal progenitor cells prevents their increase during systemic infection 36 hours following **(A)** PBS injection or **(B)** systemic *C. albicans* infection, the number of ISCs / EBs (marked with GFP, green) increases (UAS-CG7923^{RNAi}), but not when the function of Toll is reduced (UAS-Toll^{RNAi}) specifically in these cells (esg > Gal4) **(C)**. Systemic infection may also induce enhanced clustering (yellow asterisks) and morphological changes (compare white asterisks) to the ISCs / EBs, which are diminished when Toll receptor activity is reduced. All nuclei stained with DAPI (grey). Each diamond represents a counted area for a single gut taken from 3 biological repeats.

355 **FIGURE 3**

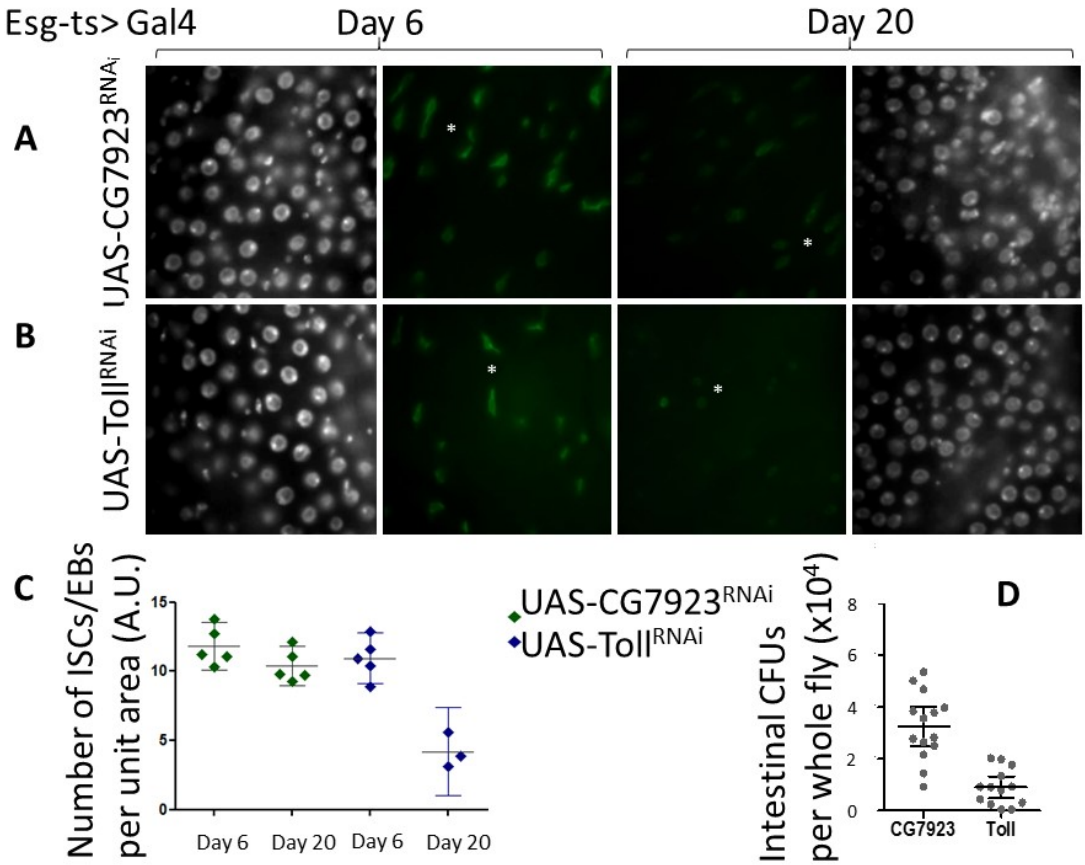

356

357 **Figure 3: The Toll receptor influences the long-term renewal of gut progenitor cells (A)** RNAi
358 knockdown of the *UAS-CG7923* was randomly chosen from the VDRC collection as a control for the
359 RNAi effect. **(B)** Using *UAS-Toll*^{RNAi} (from the same collection as *UAS-CG7923*^{RNAi}), Toll was knocked-
360 down specifically in ISCs and EBs (*esg*^{ts} > *Gal4*) of the adult gut. This led to altered morphology of
361 progenitors, where the cells generally remained rounded, rarely adopting the characteristic
362 elongated and irregular shape often observed with ISCs / EBs [compare cells marked with white
363 asterisks; ISCs / EBs are marked with GFP (green) and all nuclei stained with DAPI (grey)]. **(C)** There
364 was also a significant reduction in numbers of progenitor cells (day20 compared to all others
365 ***p<0.001, all other comparisons non-significant. **(D)** Finally, Toll knocked-down resulted in the
366 significant reduction of cultivable intestinal microbiota (CFUs) (***p<0.001) in 20-day old flies. Each
367 dot in the graphs represents a counted area for a single gut taken from 3 biological repeats. 95%
368 confidence intervals are displayed.

369

370

371

372 **FIGURE 4**

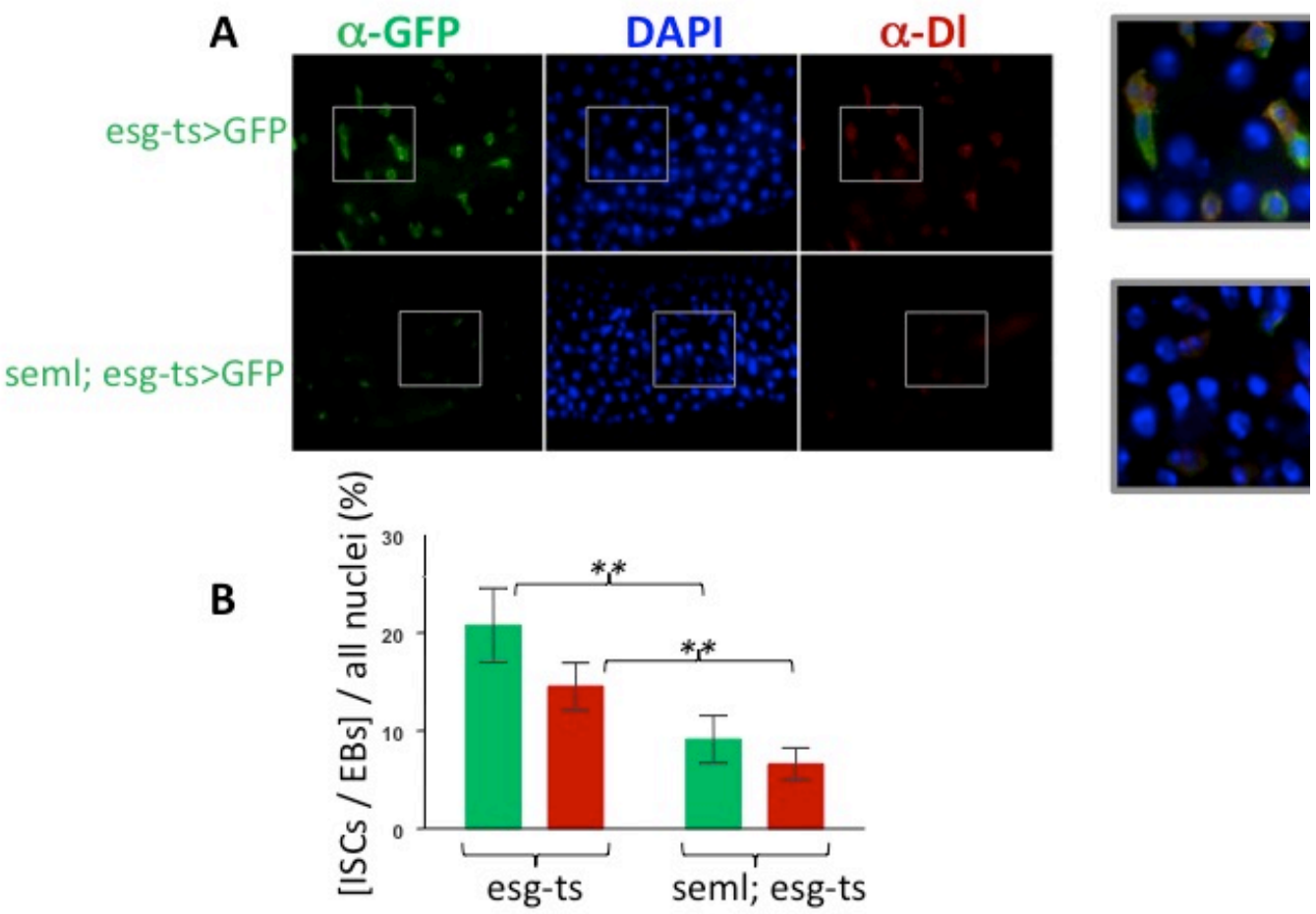

373

374 **Figure 4: PGRP-SA *seml* mutant flies have less progenitor cells. (A)** In the absence of infection, ISCs
375 (Dl positive, GFP positive) divide to produce EBs (Dl negative, GFP positive). However, in 20-day old
376 flies that were deficient for PGRP-SA this division was not observed (see also insets). **(B)**
377 Quantification of progenitor cells and ISCs showed that these were significantly reduced (**p<0.01;
378 error bars display 95% confidence interval, n=12 guts from each genotype). GFP expression was
379 directed by the UAS dependent mCD8GFP transgene, which marked the cell membranes of
380 progenitor cells including ISCs and EBs (DAPI all nuclei).

FIGURE 5

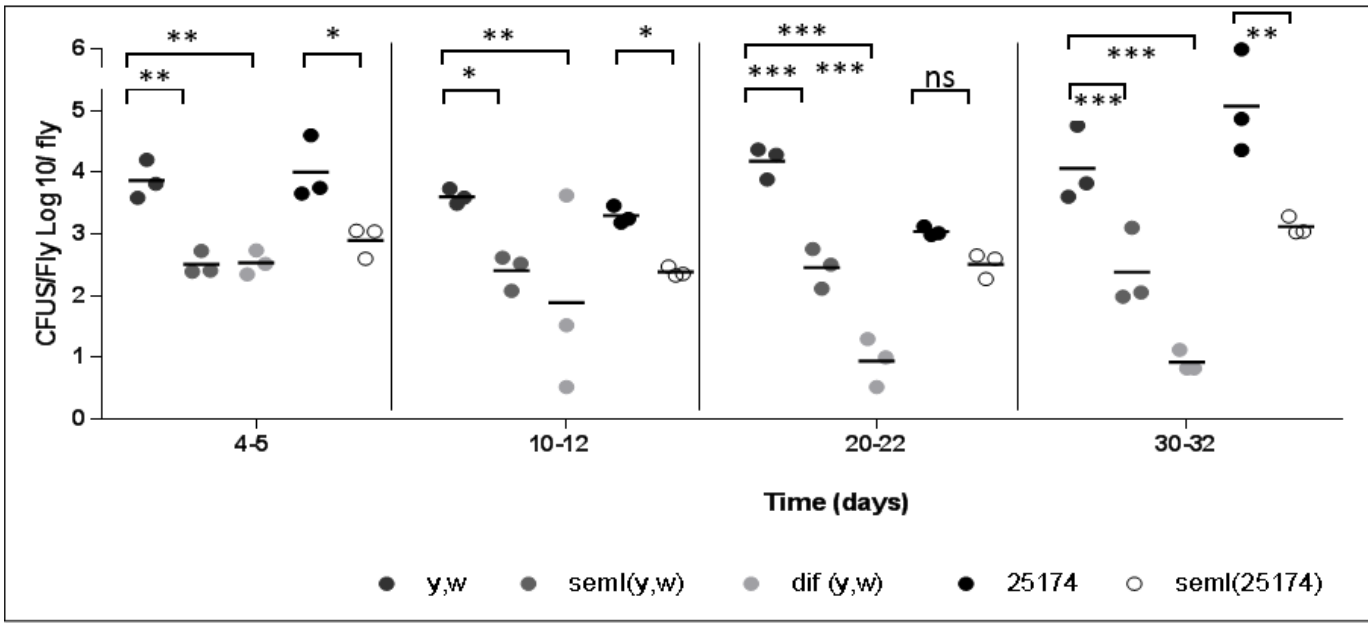

Figure 5: The effects on microbiota upon blocking of the Toll pathway. Log of CFUs /µl /fly (15 flies for each strain and each time point). 2 different WT backgrounds: *yw* and DGRP line *25174*, *PGRP-SA*^{seml} mutants in both backgrounds and *dif*^{1} mutant in *yw* used. Plates incubated overnight at 30^{o}C. *P<0.01, **P<0.01, ***P<0.001.

FIGURE 6

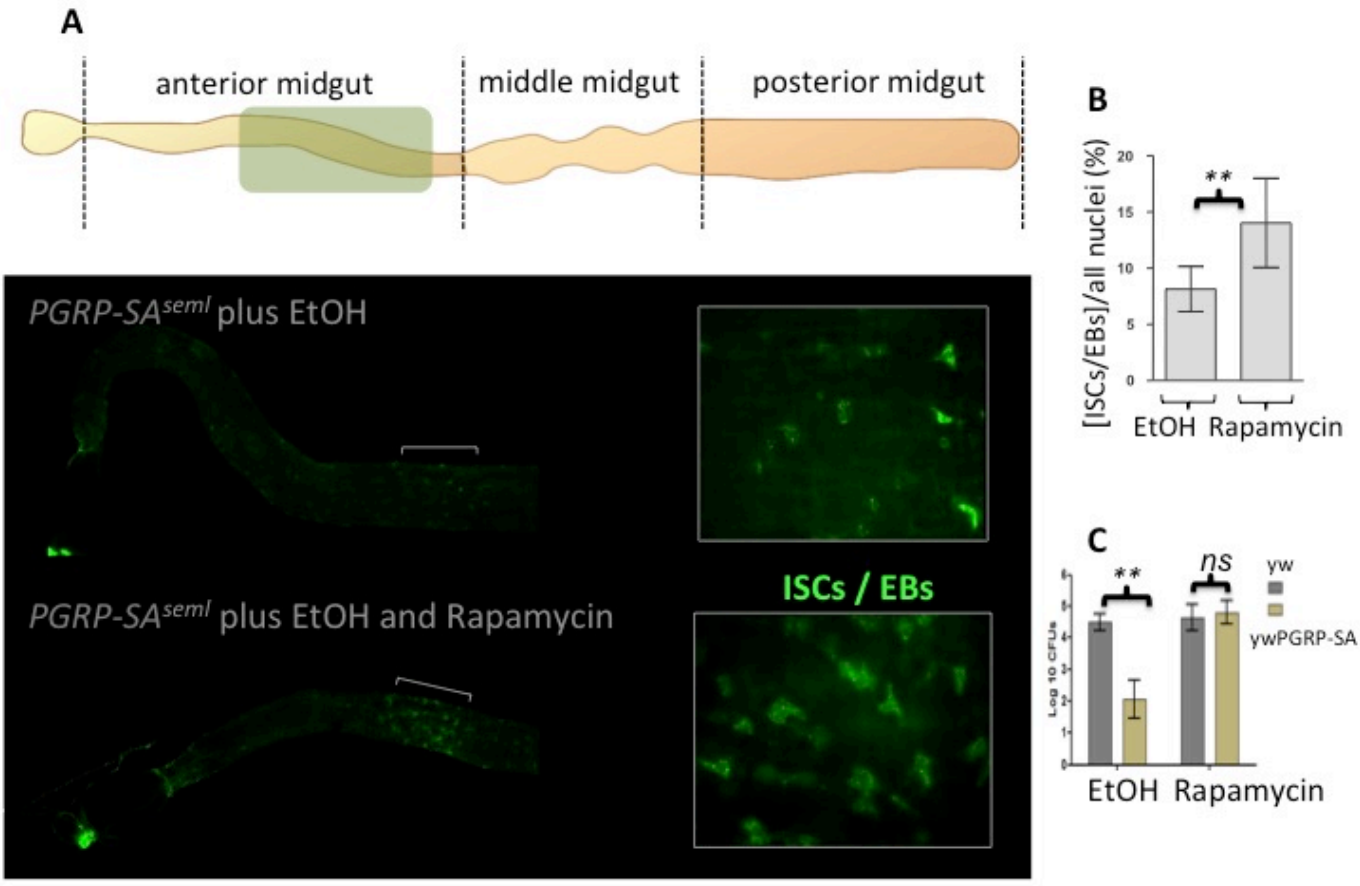

Figure 6: Rapamycin restores progenitor cells in *PGRP-SA^{seml}* flies. (A) Anterior midgut progenitor cells were increased when *PGRP-SA^{seml}* flies were given rapamycin compared to the vehicle control (EtOH). **(B)** This was verified in measurements comparing intestinal progenitor numbers between EtOH and Rapamycin in EtOH in *PGRP-SA^{seml}* guts. **(C)** This restored the gut microbiota to the levels of the *yw* genetic background. For all panels: **p<0.001, ns=non-significant, error bars represent 95% confidence levels, n=30 guts for each treatment/genotype.

406

407

408

409

410

411

412

413

414

415

416

417

418

419

420

421

422

423

424

425

426 **FIGURE 7**

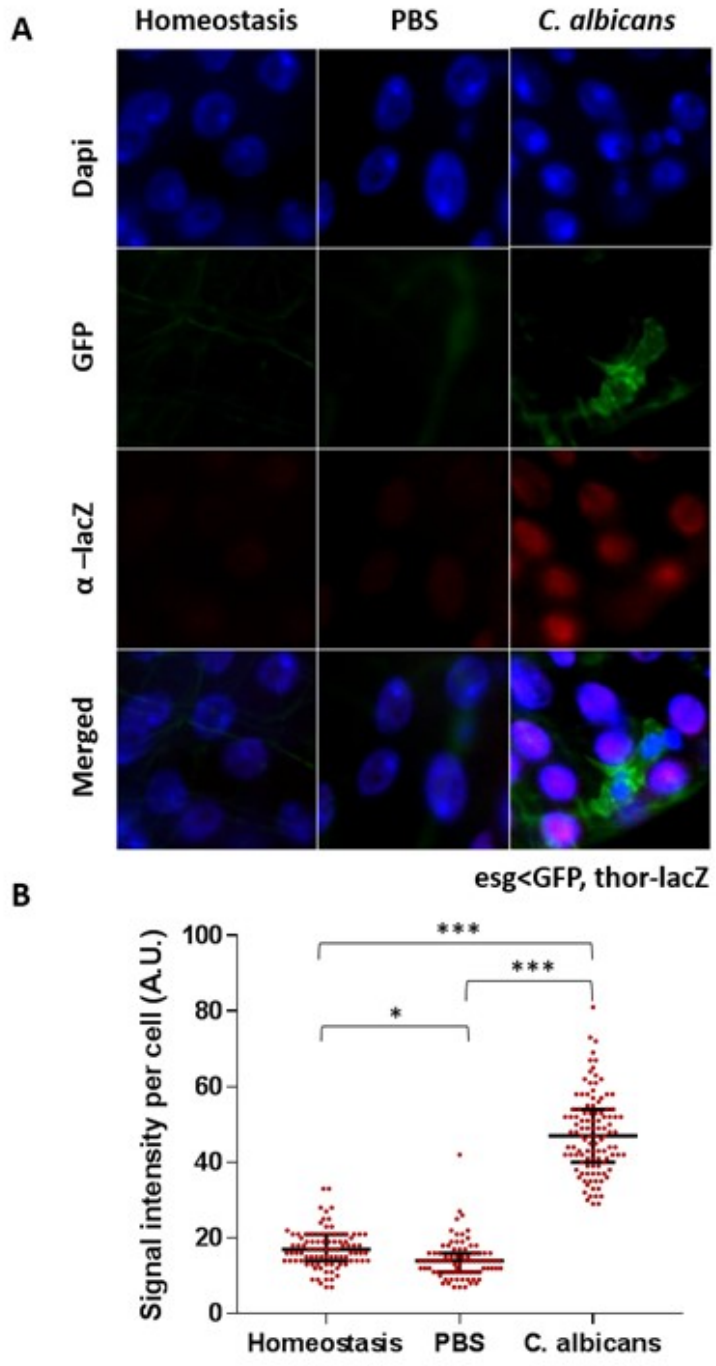

427

428 **Figure 7: Systemic infection of *C. albicans* activates FOXO-dependent transcription in enterocytes.**

429 **(A)** Flies injected with *C. albicans* were sampled 36h post-infection and compared to non-treated

430 (homeostasis) or those injected with PBS (sterile injury). Gut cells stained with DAPI (blue), anti-β-

431 galactosidase (red) and anti-GFP expressing cells (marking both ISCs and EBs). Shown are

representative images from the anterior mid-gut taken at 63x. **(B)** Quantification of *thor-LacZ* expression upon systemic infection. Intensity measured using ImageJ, subtraction of the background was performed for all samples. Ten guts were analysed (approximately 50 cells analysed per gut). 95% confidence intervals displayed, ***P<0.001, *P<0.1.

FIGURE 8

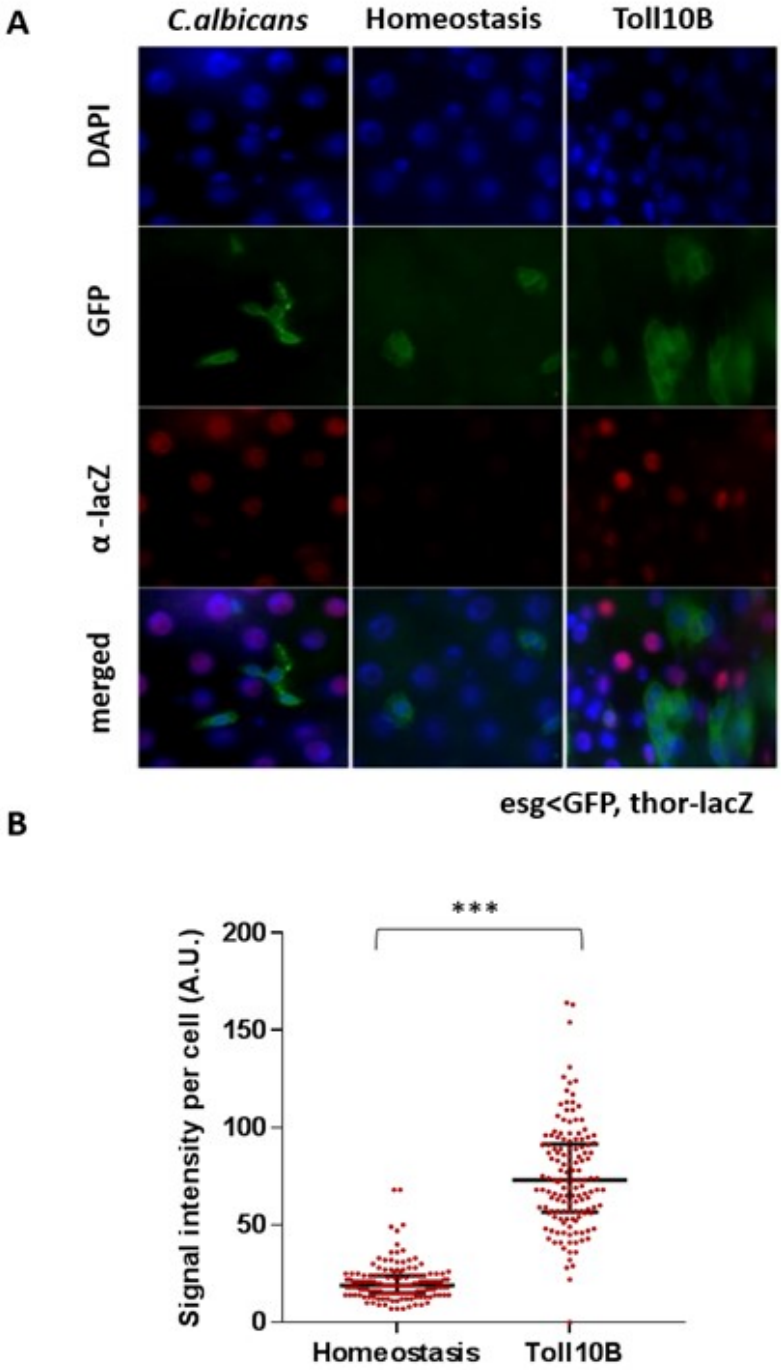

Figure 8: FOXO-dependent transcription in Toll10B flies. . **(A)** Flies injected with *C. albicans* were sampled 36h post-infection and compared to non-treated (homeostasis) or those expressing Toll10B.

459 Gut cells stained with DAPI (blue), anti-β-galactosidase (red) and anti-GFP expressing cells (marking
460 both ISCs and EBs). Shown are representative images from the anterior mid-gut taken at 63x. Two
461 left hand columns show *thor-lacZ; esg^{ts}<GFP* flies; right column *thor-lacZ; esg^{ts}<GFP* flies also express
462 the *UAS-Toll10B* transgene **(B)** Quantification of *thor-LacZ* expression upon systemic infection.
463 Intensity measured using ImageJ, subtraction of the background was performed for all samples. Ten
464 guts were analysed (approximately 50 cells analysed per gut). 95% confidence intervals displayed,
465 ***P<0.001.